PROCEEDINGS OF THE ROYAL SOCIETY A MATHEMATICAL, PHYSICAL & ENGINEERING SCIENCES

Effects of Hall and ion–slip currents on magneto–micropolar fluid and heat transfer over a non –isothermal stretching sheet with suction and blowing

M. A. Seddeek

Proc. R. Soc. Lond. A 2001 **457**, doi: 10.1098/rspa.2001.0847, published 8 December 2001

10.1098/rspa.2001.0847

THE ROYAL SOCIETY

Effects of Hall and ion-slip currents on magneto-micropolar fluid and heat transfer over a non-isothermal stretching sheet with suction and blowing

By M. A. Seddeek

Department of Mathematics, Faculty of Science, Helwan University, Ain Helwan, PO Box 11795, Cairo, Egypt

Received 3 January 2001; accepted 1 May 2001

In this work, the effects of Hall and ion-slip currents on the steady magneto-micropolar of a viscous incompressible and electrically conducting fluid is analysed using the theory of micropolar fluids formulated by Eringen. Heat transfer from a stretching sheet to a micropolar fluid is also considered. The derived fundamental equations on the assumption of small magnetic Reynolds number are solved numerically by employing the shooting method. Expressions for the velocities and temperature fields are obtained, and the effects of the various parameters of the problem, e.g. the magnetic parameter, Hall parameter, ion-slip parameter, mass transfer parameter and power-law exponent parameter, are discussed through graphs.

Keywords: magneto-micropolar; Hall currents; stretching; sheet; suction; blowing

1. Introduction

The study of magneto-micropolar fluid flows in a slip-flow regime with Hall and ion-slip currents has important engineering applications, e.g. in power generators, magnetohydrodynamic (MHD) accelerators, refrigeration coils, transmission lines, electric transformers and heating elements. The theory of micropolar fluids that displays the effects of local rotary inertia and coupled stresses was formulated by Eringen (1966). The theory can be used to explain the flow of colloidal fluids, liquid crystals, etc. The present problem finds application in MHD generators with neutral fluid seeding in the form of rigid microinclusions. Also, many industrial applications involve fluids as a working medium, and in such applications unclean fluids (i.e. clean fluid plus interspersed particles) are the rule and clean fluids an exception. Control of convection is also important in many of these non-isothermal applications. To the knowledge of the author no paper seems to address itself to the problem of magneto-micropolar fluids, i.e. effects of Hall and ion-slip currents on electrically conducting micropolar fluids in the presence of a strong magnetic field. This will will be the focus of this paper. Literature on magneto-micropolar fluid and heat transfer is very extensive due to its technical importance in the scientific community. Some literature surveys and reviews of pertinent work in this field are documented by Ahmadi & Shahinpoor (1974), who recently analysed the universal stability of magneto-micropolar fluid

motions. Magneto-micropolar fluid motion, on the convergence rate of the spectral Galerkin approximations, was analysed by Rojas-Medar (1997). Also, Ortega-Torres & Rojas-Medar (1998) studied the initial-value problem for the equations of magneto-micropolar fluid in a time-dependent domain. Pop & Watanabe (1994) studied the effects of Hall current on MHD free convection flow past a semi-infinite vertical flat plate. Ram (1995) studied the effects of Hall and ion-slip currents on free convective heat-generating flow in a rotating fluid. The heat and mass transfer on a stretching sheet with suction and injection was investigated by Gupta & Gupta (1977). The solution of heat transfer to micropolar fluid from a non-isothermal stretching sheet with injection was introduced by Hady (1996). Boundary-layer flow on continuous surfaces is an important type of flow occurring in a number of technical processes. The continuous surface concept was introduced by Sakiadis (1961). Soundalgeker & Takhar (1983) studied the flow and heat transfer past a continuously moving flat plate in a micropolar fluid. Gorla & Ameri (1985) recently analysed the fluid mechanics and heat transfer characteristics of the boundary-layer flow of a laminar micropolar fluid on a continuous moving cylinder.

In the present work, the aim is to investigate the Hall and ion-slip current effects of neutral seeding of the fluid, in the form of introducing relatively rigid microelements in the fluid which is moving in the presence of a magnetic field. A linear micropolar fluid as presented by Eringen (1966) is assumed to represent the model of the fluid under consideration. We have chosen to call the fluid under discussion a magneto-micropolar fluid. The criteria for Hall and ion-slip current effects on magneto-micropolar fluid and heat transfer from a non-isothermal stretching sheet with suction and blowing are then obtained. Numerical solutions are presented for the velocities, microrotation and temperature fields by using the shooting method. The effects of the various parameters of the problem, e.g. the magnetic field parameter M, Hall parameter β_{e}, ion-slip parameter β_{i}, mass transfer parameter f_{w}, and power-law exponent parameter γ are discussed.

2. Governing equations

Let us consider a steady, incompressible, micropolar and electrically conducting fluid flowing past a horizontal stretching sheet in the x-direction, which issues from a thin slit, as found in polymer-processing applications. The flow is subjected to a transverse strong magnetic field $\boldsymbol{B}_0$ with constant intensity along the y-axis. The induced magnetic field is neglected, since the magnetic Reynolds number is assumed to be very small. In general, for an electrically conducting fluid, Hall and ion-slip current significantly affect the flow in the presence of a strong magnetic field. The effect of the Hall current gives rise to a force in the z-direction, which induces a cross flow in that direction and hence the flow becomes three-dimensional. To simplify the problem, we assume that there is no variation of flow or heat-transfer quantities in the z-direction.

The governing equations within the boundary-layer approximation may be written as

$$\frac{\partial u}{\partial x} + \frac{\partial v}{\partial y} = 0, \tag{2.1}$$

$$u\frac{\partial u}{\partial x}+v\frac{\partial u}{\partial y}=\nu\frac{\partial^2 u}{\partial y^2}+K_1\frac{\partial N}{\partial y}-\frac{\boldsymbol{B}_0}{\rho}\boldsymbol{J}_z, \tag{2.2}$$

$$u\frac{\partial w}{\partial x}+v\frac{\partial w}{\partial y}=\nu\frac{\partial^2 w}{\partial y^2}+\frac{\boldsymbol{B}_0}{\rho}\boldsymbol{J}_x, \tag{2.3}$$

$$G_1\frac{\partial^2 N}{\partial y^2}-2N-\frac{\partial u}{\partial y}=0, \tag{2.4}$$

$$u\frac{\partial T}{\partial x}+v\frac{\partial T}{\partial y}=k\frac{\partial^2 T}{\partial y^2}+\frac{\nu}{C_p}\left(\frac{\partial u}{\partial y}\right)^2, \tag{2.5}$$

where u, v and w are the velocity components associated with the directions of increasing the coordinates x, y and z, respectively.

The boundary conditions are given by

$$\left.\begin{array}{lllll} y=0: & u=Bx, & v=v_{\mathrm{w}}, & w=0, & N=0, \quad (T-T_\infty)=Ax^\gamma, \\ & y\to\infty: & u\to 0, & w\to 0, & N\to 0, \quad T\to T_\infty. \end{array}\right\} \tag{2.6}$$

In the previous equations, A, B and γ are constant.The equation of conservation of electric charge $\nabla\cdot\boldsymbol{J}=0$ gives $\boldsymbol{J}_y=\text{const}$. This constant is zero, since $\boldsymbol{J}_y=\boldsymbol{0}$ at the surface. Thus $\boldsymbol{J}_y=\boldsymbol{0}$ everywhere in the flow. The expressions for the current-density components $\boldsymbol{J}_x$ and $\boldsymbol{J}_z$ as obtained from the generalized Ohm's law (Sutton & Sherman 1965) in the absence of electric field are given by

$$\boldsymbol{J}_x=\frac{\sigma\beta_{\mathrm{e}}\boldsymbol{B}_0}{\alpha_{\mathrm{e}}^2+\beta_{\mathrm{e}}^2}u-\frac{\sigma\alpha_{\mathrm{e}}\boldsymbol{B}_0}{\alpha_{\mathrm{e}}^2+\beta_{\mathrm{e}}^2}w,$$

$$\boldsymbol{J}_z=\frac{\sigma\alpha_{\mathrm{e}}\boldsymbol{B}_0}{\alpha_{\mathrm{e}}^2+\beta_{\mathrm{e}}^2}u+\frac{\sigma\beta_{\mathrm{e}}\boldsymbol{B}_0}{\alpha_{\mathrm{e}}^2+\beta_{\mathrm{e}}^2}w,$$

where $\alpha_{\mathrm{e}}=1+\beta_{\mathrm{i}}\beta_{\mathrm{e}}$.

We further define the following similarity variables:

$$\left.\begin{array}{lll} \eta=\left(\dfrac{B}{\nu}\right)^{1/2}y, & \psi=(B\nu)^{1/2}xf(\eta), & w=(B\nu)^{1/2}xg(\eta), \\ N=\left(\dfrac{B^3}{\nu}\right)^{1/2}xh(\eta), & \theta=\dfrac{T-T_\infty}{T_{\mathrm{w}}-T_\infty}, & \\ \nu=\dfrac{\mu+K}{\rho}, & K_1=\dfrac{K}{\rho}, & u=\dfrac{\partial\psi}{\partial y}, \quad v=-\dfrac{\partial\psi}{\partial x}. \end{array}\right\} \tag{2.7}$$

Substituting equation (2.7) into (2.1)–(2.5), we have

$$f'''+ff''-(f')^2=-N_1h'-\frac{2M}{\alpha_{\mathrm{e}}^2+\beta_{\mathrm{e}}^2}(\alpha_{\mathrm{e}}f'+\beta_{\mathrm{e}}g), \tag{2.8}$$

$$g''-f'g+fg'=\frac{2M}{\alpha_{\mathrm{e}}^2+\beta_{\mathrm{e}}^2}(\alpha_{\mathrm{e}}g-\beta_{\mathrm{e}}f'), \tag{2.9}$$

$$Gh''-(2h+f'')=0, \tag{2.10}$$

$$\frac{1}{pr}\theta''+f\theta'+Ecf''^2-\gamma f'\theta=0. \tag{2.11}$$

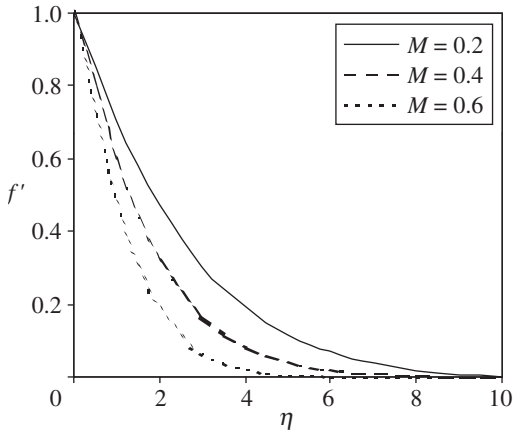

Figure 1. Distribution of velocity profiles along the plate at $\beta_e = 5$, $\beta_i = 0.4$, $f_w = 0$ and $\gamma = 0.4$.

In the above equations a prime denotes differentiation with respect to η only. The transformed boundary conditions are given by

$$\left.\begin{aligned} f(0) = f_w, \quad f'(0) = 1, \quad g(0) = 0, \quad h(0) = 0, \quad \theta(0) = 1, \\ f'(\infty) = 0, \quad g(\infty) = 0, \quad h(\infty) = 0, \quad \theta(\infty) = 0, \end{aligned}\right\} \tag{2.12}$$

where

$$N_1 = \frac{K_1}{\nu}, \qquad G = \frac{G_1 B}{\nu}, \qquad f_w = \frac{v_w}{(B\nu)^{1/2}}, \qquad Ec = \frac{U^2}{C_p(T_w - T_\infty)}.$$

It is important to note that the mass-transfer parameter f_w is positive for injection and negative for suction.

The shooting method is employed, and we use the symbolic computation software MATHEMATICA to solve the initial-value problems. Hence, equations (2.8)–(2.11) reduce to a system of nonlinear equations with variable coefficients which could be solved by the shooting method to obtain f', g, h and θ.

3. Results and discussion

To study the behaviour of the velocities, angular velocity and temperature profiles, curves are drawn for various values of the parameters that describe the flow. The results obtained for steady flow are displayed in figures 1–19 for $Pr = 0.72$, $Ec = 0.02$, $N_1 = 0.2$ and $G = 2$ at different values of the magnetic field parameter M, the Hall parameter β_e, the ion-slip parameter β_i, the mass transfer parameter f_w and the power-law exponent parameter γ.

It is seen from figures 1–4 that, as expected, the velocity profiles along the f' and the angular velocity h decrease monotonically, while the velocity profiles across the plate g and the temperature profiles θ increase with increasing magnetic parameter M. This decrease of f' happens because of an accelerating force, which acts in a direction parallel to the x-axis when Hall and ion-slip currents are absent.

Figures 5–8 show the f', g, h and θ profiles at different values of β_e. We see that f' and h increase with increasing parameter β_e. Figure 6 shows that the induced flow in

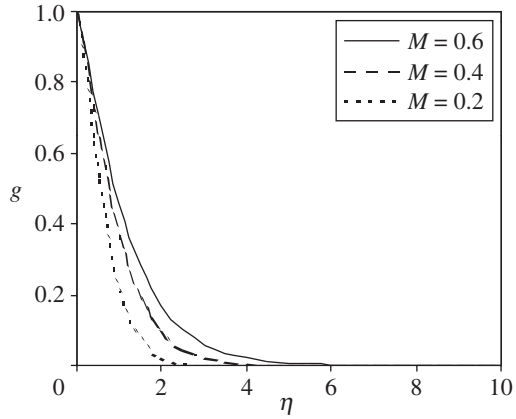

Figure 2. Distribution of velocity profiles across the plate at $\beta_e = 5$, $\beta_i = 0.4$, $f_w = 0$ and $\gamma = 0.4$.

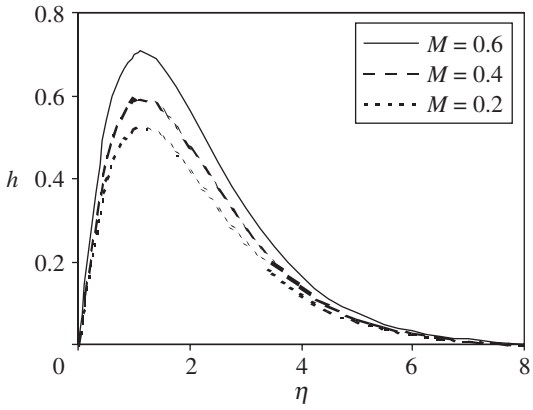

Figure 3. Distribution of angular velocity profiles at $\beta_e = 5$, $\beta_i = 0.4$, $f_w = 0$ and $\gamma = 0.4$.

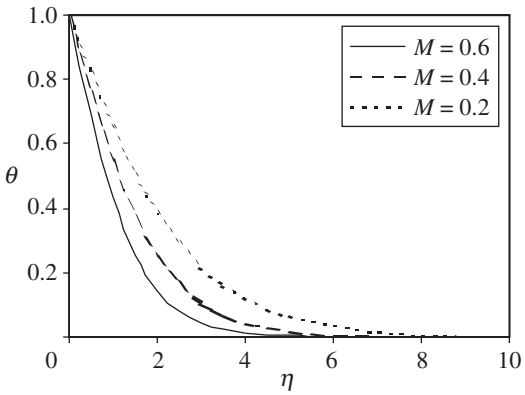

Figure 4. Distribution of temperature profiles at $\beta_e = 5$, $\beta_i = 0.4$, $f_w = 0$ and $\gamma = 0.4$.

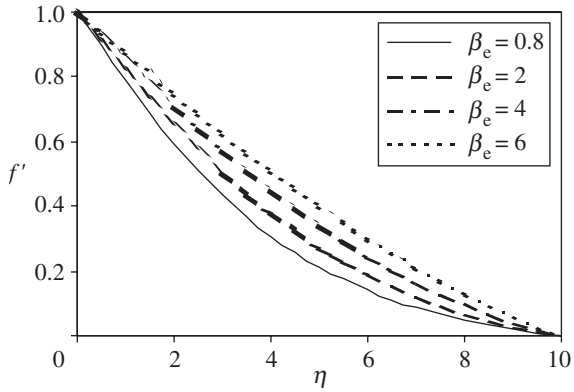

Figure 5. Distribution of velocity profiles along the plate at $M = 0.3$, $\beta_i = 0.4$, $f_w = 0$ and $\gamma = 0.4$.

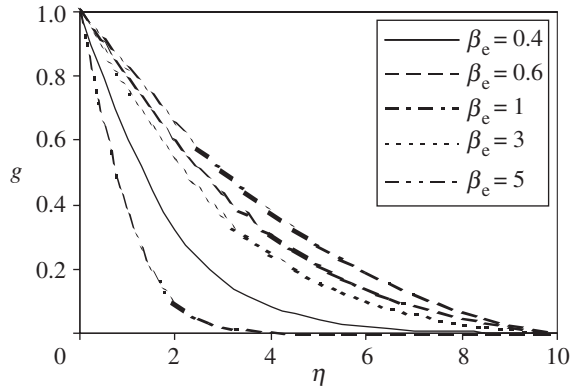

Figure 6. Distribution of velocity profiles across the plate at $M = 0.3$, $\beta_i = 0.4$, $f_w = 0$ and $\gamma = 0.4$.

the z-direction begins to develop as the Hall parameter β_e increases in the interval $0 \leqslant \beta_e \leqslant 1$ and decreases for $\beta_e > 1$.

Figures 9–12 display the variation of f', g, h and θ at different values of the ion-slip parameter β_i. It is seen that the f', h and θ profiles increase as the ion-slip parameter increases, while the induced flow in the z-direction decreases with increasing the parameter β_i.

The effect of surface mass transfer on the dimensionless velocity, the velocity across the plate, the angular velocity and the temperature distributions is displayed in figures 13–16. The effect of suction is to make the velocities and temperature distributions more uniform within the boundary layer. The increasing values of the suction parameter move the location of the maximum value of the micro-rotation away from the surface. Figure 17 shows the velocity f' for several values of γ, and we see that the velocity f' decreases with increasing parameter γ. On the other hand, figure 18 shows that the induced flow in the z-direction increases with increasing parameter γ. Figure 19 shows the temperature distribution for several values of γ. We observe that the direction of heat flow changes for some negative values of γ, and a zero temperature gradient with the boundary layer exists for these values of γ.

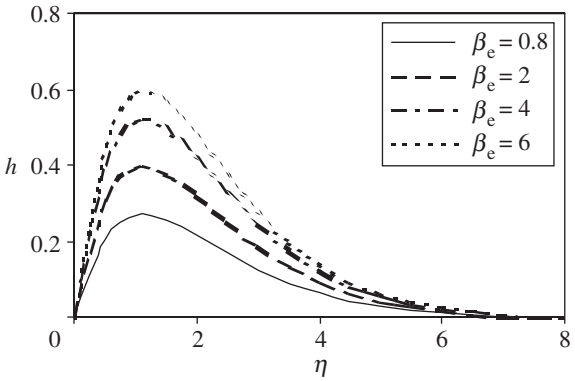

Figure 7. Distribution of angular velocity profiles at $M = 0.3$, $\beta_i = 0.4$, $f_w = 0$ and $\gamma = 0.4$.

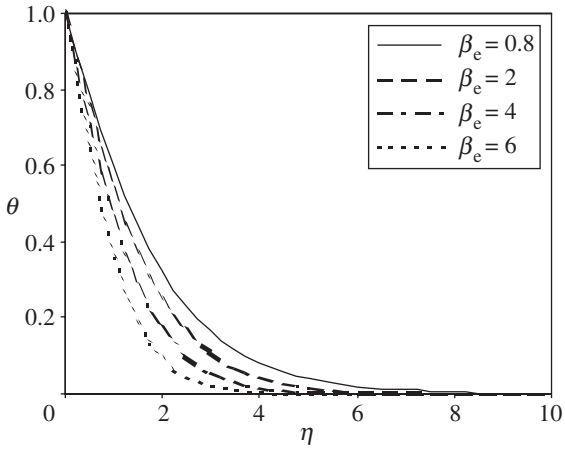

Figure 8. Distribution of temperature profiles at $M = 0.3$, $\beta_i = 0.4$, $f_w = 0$ and $\gamma = 0.4$.

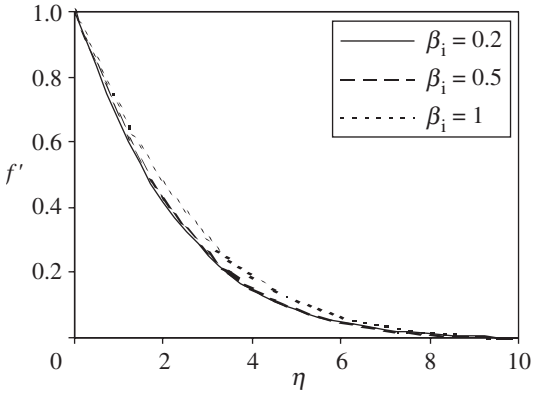

Figure 9. Distribution of velocity profiles along the plate at $\beta_e = 5$, $M = 0.3$, $f_w = 0$ and $\gamma = 0.5$.

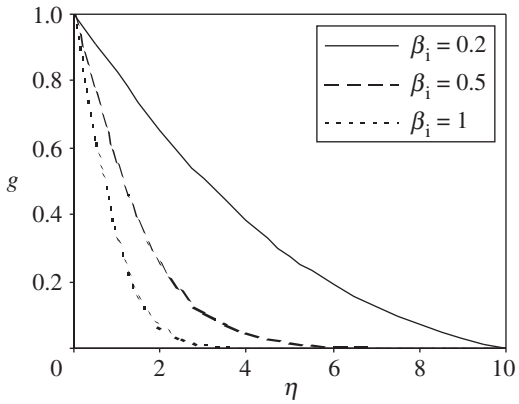

Figure 10. Distribution of velocity profiles across the plate at $\beta_e = 5$, $M = 0.3$, $f_w = 0$ and $\gamma = 0.5$.

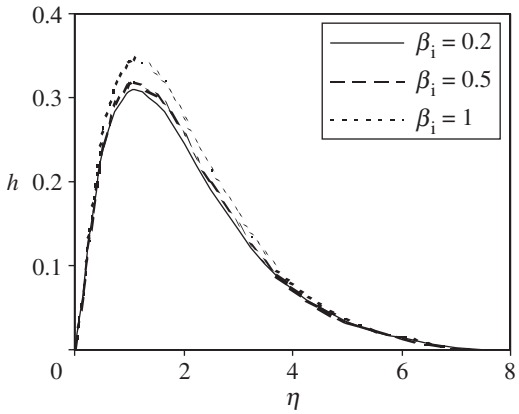

Figure 11. Distribution of angular velocity profiles at $\beta_e = 5$, $M = 0.3$, $f_w = 0$ and $\gamma = 0.5$.

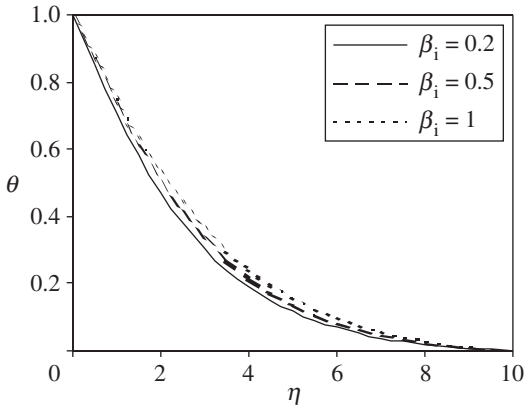

Figure 12. Distribution of temperature profiles at $\beta_e = 5$, $M = 0.3$, $f_w = 0$ and $\gamma = 0.5$.

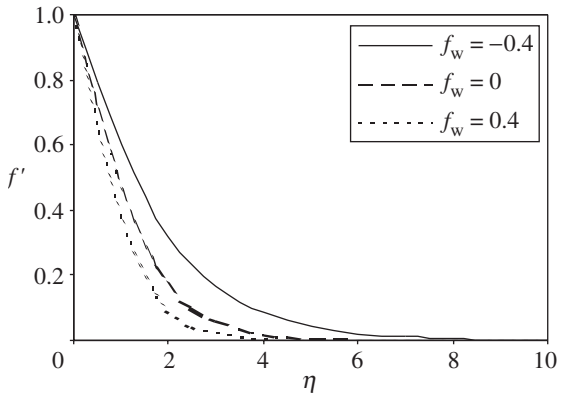

Figure 13. Distribution of velocity profiles along the plate at $\beta_e = 5$, $\beta_i = 0.4$, $M = 0.3$ and $\gamma = 0.5$.

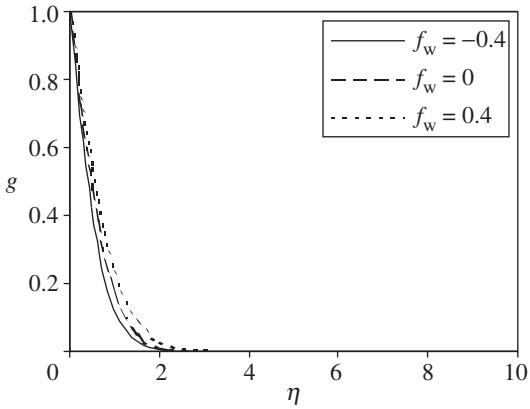

Figure 14. Distribution of velocity profiles across the plate at $\beta_e = 5$, $\beta_i = 0.4$, $M = 0.3$ and $\gamma = 0.5$.

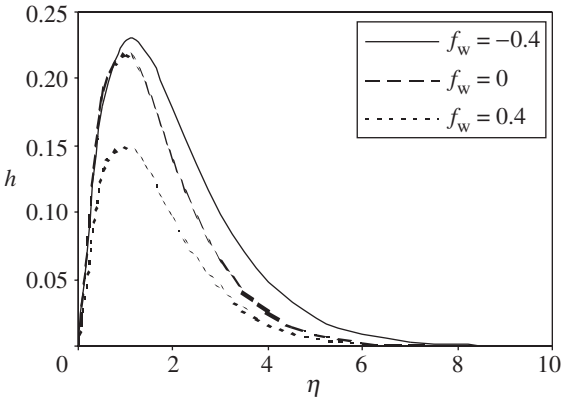

Figure 15. Distribution of angular velocity profiles at $\beta_e = 5$, $\beta_i = 0.4$, $M = 0.3$ and $\gamma = 0.5$.

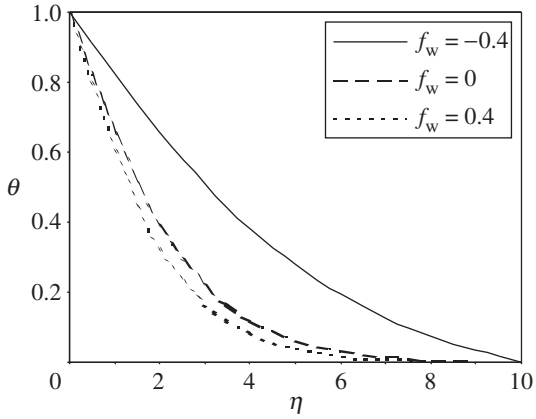

Figure 16. Distribution of temperature profiles at $\beta_e = 5$, $\beta_i = 0.4$, $M = 0.3$ and $\gamma = 0.5$.

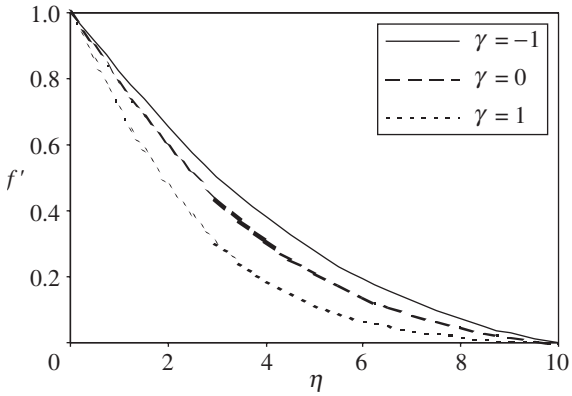

Figure 17. Distribution of velocity profiles along the plate at $\beta_e = 5$, $\beta_i = 0.4$, $f_w = 0$ and $M = 0.3$.

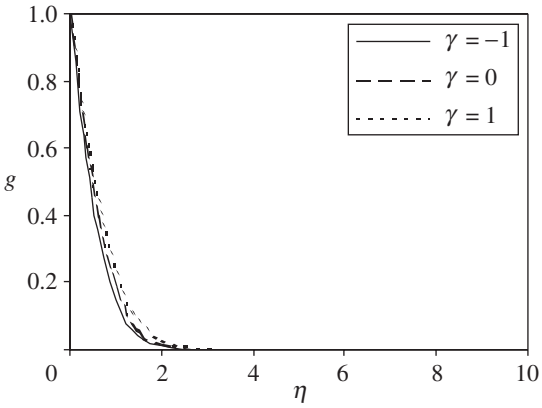

Figure 18. Distribution of velocity profiles across the plate at $\beta_e = 5$, $\beta_i = 0.4$, $f_w = 0$ and $M = 0.3$.

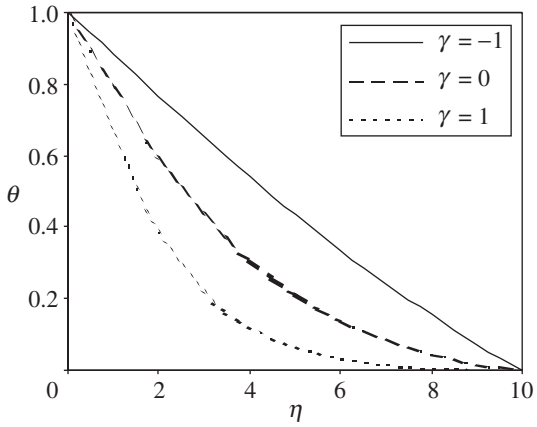

Figure 19. Distribution of temperature profiles at $\beta_e = 5$, $\beta_i = 0.4$, $f_w = 0$ and $M = 0.3$.

Finally, clean fluids with interspersed particles are used in many industrial applications and thus micropolar fluid convection is important and also applicable where unclean fluids are used as a working medium. The results of the present study also indicate that unclean fluids may, in fact, be preferable to clean fluids in applications where control of convection is important.

I thank Professor Walter Wyss of the University of Colorado, Boulder, CO, USA, for his support in reviewing and revising this work. I am also grateful to Dr Rabia Djellouli of the University of Colorado for helping me with some of the computations done in this research.

Nomenclature

Ec	Eckert number
f	dimensionless velocity
g	dimensionless velocity across the plate
h	dimensionless micro-rotation
G, N_1	dimensionless material parameters
j	micro-inertia per unit mass
K	thermal conductivity
N	angular velocity
Nu	Nusselt number
Pr	Prandtl number
Re	Reynolds number
C_p	specific heat at constant pressure
β_e	Hall parameter
β_i	ion-slip parameter
σ	electrical conductivity
$\boldsymbol{B}_0$	strong magnetic field
M	magnetic parameter
T	temperature

u	velocity in x-direction
v	velocity in y-direction
w	velocity in z-direction
U	surface velocity
x	distance along the surface
y	distance normal to the surface
ν	kinematic viscosity
ρ	density of the fluid
θ	dimensionless temperature
γ	power-law exponent

subscripts

w	conditions at the surface
∞	conditions far away from the surface

References

Ahmadi, G. & Shahinpoor, M. 1974 Universal stability of magneto-micropolar fluid motions. *Int. J. Engng Sci.* **12**, 657–663.

Eringen, A. C. 1966 Theory of micropolar fluids. *J. Math. Mech.* **16**, 1.

Gorla, R. S. R. & Ameri, A. 1985 Boundary layer flow of a micro-polar fluid on a continuous moving cylinder. *Acta Mech.* **53**, 203.

Gupta, P. S. & Gupta, A. S. 1977 Heat and mass transfer on a stretching sheet with suction and blowing. *Can. J. Chem. Engng* **55**, 744.

Hady, F. M. 1996 Short communication on the solution of heat transfer to micropolar fluid from a non-isothermal stretching sheet with injection. *Int. J. Numer. Meth. Heat Fluid Flows* **6**, 99–104.

Ortega-Torres, E. & Rojas-Medar, M. 1998 The initial value problem for the equations of magneto-micropolar fluid in a time-dependent domain. *Mat. Contemp.* **15**, 259–281.

Pop, I. & Watanabe, T. 1994 Hall effects on MHD free convection about a semi-infinite vertical flat plate. *Int. J. Engng Sci.* **32**, 1903–1911.

Ram, P. C. 1995 Effects of Hall and ion-slip currents on free convective heat generating flow in a rotating fluid. *Int. J. Energy Res.* **19**, 371–376.

Rojas-Medar, M. A. 1997 Magneto-micropolar fluid motion: existence and uniqueness of a strong solution. *Math. Nachr.* **188**, 301–319.

Sakiadis, B. C. 1961 Boundary layer behavior on continuous solid surface: the boundary layer on a continuous flat surface. *AIChE J.* **7**, 221.

Soundalgeker, V. M. & Takhar, H. S. 1983 Boundary layer flow of a micro-polar fluid on a continuous moving plate. *Int. J. Engng Sci.* **21**, 961.

Sutton, G. W. & Sherman, A. 1965 *Engineering magnetohydrodynamics*. New York: McGraw-Hill.